energies

MDPI

Article

Application of Silver Nanoparticles Supported over Mesoporous Carbon Produced from Sustainable Sources as Catalysts for Hydrogen Production

Erik Biehler [1,2], Qui Quach [1,2] and Tarek M. Abdel-Fattah [1,2,*]

[1] Applied Research Center, Thomas Jefferson National Accelerator Facility, Newport News, VA 23606, USA; erik.biehler@cnu.edu (E.B.); qui.quach.13@cnu.edu (Q.Q.)
[2] Department of Molecular Biology and Chemistry, Christopher Newport University, Newport News, VA 23606, USA
* Correspondence: fattah@cnu.edu

Abstract: The growing population and increasingly competitive economic climate have increased the demand for alternative fuel sources, with hydrogen being one of the more viable options. Many metal hydrides, including sodium borohydride, are capable of releasing hydrogen stored within chemical bonds when reacted with water, but the rate of generation is slow and therefore necessitates a catalyst. Silver nanoparticles, which were chosen due to their known catalytic activity, were synthesized from sodium citrate and were embedded in mesoporous carbon to form a nano-composite catalyst (Ag-MCM). This composite was characterized via Transmission Electron Microscopy (TEM), X-ray Diffraction (XRD), and Scanning Electron Microscopy/Energy-Dispersive X-ray Spectroscopy (SEM/EDS). Catalytic testing showed that the catalytic activity for the Ag-MCM catalyst increased with increasing $NaBH_4$ concentration, low pH, and high temperatures. The Ag-MCM catalyst resulted in the activation energy at 15.6 kJ mol^{-1}, making it one of the lowest seen activation energies for inorganic catalysts. Lastly, the Ag-MCM catalysts showed stability, producing, on average, 20.0 mL per trial for five consecutive trials. This catalytic ability along with the cheap, carbon-based backbone that is made from readily available corn starch, makes it a promising catalyst for the hydrolysis of $NaBH_4$.

Keywords: silver nanoparticles; mesoporous carbon; sustainable source; hydrogen production

Citation: Biehler, E.; Quach, Q.; Abdel-Fattah, T.M. Application of Silver Nanoparticles Supported over Mesoporous Carbon Produced from Sustainable Sources as Catalysts for Hydrogen Production. *Energies* **2024**, *17*, 3327. https://doi.org/10.3390/en17133327

Academic Editor: Asif Ali Tahir

Received: 25 May 2024
Revised: 17 June 2024
Accepted: 1 July 2024
Published: 7 July 2024

1. Introduction

The world is going through a major energy crisis that is led by the overreliance on nonrenewable fuels, such as coal, natural gas, and oil. These fossil fuels are formed from the remains of previously living organisms, with 33%, 29%, and 24% of the world's fuel sources being from oil, coal, and natural gas, respectively [1]. It is also predicted that within 25, 97, and 27 years, all oil, coal, and natural gas, respectively, will run out if current consumption rates continue [2]. Along with these fuels being nonrenewable, they also negatively impact the environment. The combustion of fossil fuels releases UV-radiation-absorbing gases, known as Greenhouse Gases (with CO_2 being the most common), which release excess heat that causes the surface to warm. A concerning trend in CO_2 emissions is being monitored with an accelerating emission rate from 1.1% from 1990 to 1999 to 3% from 2000 to 2004 [3]. Fortunately, there are several types of renewable energy sources and alternative fuels that could remedy these issues, with hydrogen fuel being a viable option.

Hydrogen fuel is an alternative type of fuel that has shown great potential in solving the world's energy crisis. Hydrogen is not only one of the most abundant known substances, but when combusted in a fuel cell, it is one of the most energy-dense fuels. When compared to the energy generation of gasoline (47.4 J/kg), the energy released from hydrogen combustion is nearly three times as much (141.9 J/kg), making it a significantly

better option [4]. Furthermore, hydrogen is fairly simple to generate, with a common generation method being from the reaction of metal borides and water, with the reaction involving sodium borohydride ($NaBH_4$), as seen in Equation (1).

$$NaBH_4 + 2H_2O \rightarrow 4H_2 + NaBO_2 + 300\ kJ \quad (1)$$

When hydrogen is used for fuel purposes, the only byproduct in terms of its reaction for energy is water, so its environmental impact is minimal, and the recycled water could be used for more reactions. The reaction that occurs within hydrogen fuel cells can be seen in Equation (2).

$$H_2 + ½H_2 \rightarrow H_2O \quad (2)$$

One of the biggest downsides for this hydrogen generation reaction is the slow rate of reaction between metal hydrides and water. This makes it so a catalyst is necessary in order to make the fuel source more viable. There are a variety of different types of catalysts, but one class of materials that shows potential lies in that of nanomaterials.

Since the discovery of nanomaterials, strides have been taken to discover their many unique properties, with one such being their catalytic properties. One family of nanomaterial is a type of porous carbon known as Mesoporous Carbon Materials (MCMs) [5]. In general, the different types of porous carbons are characterized by their differences in pore sizes, with Mesoporous Carbon Materials having a pore size of between 2 and 50 nm, while Microporous and Macroporous carbon have smaller and larger pore sizes, respectively [6,7]. Mesoporous Carbon Materials can further be classified into two smaller categories—ordered mesoporous carbon (OMC) and non-ordered mesoporous carbon [8]. OMCs exhibit uniform pore distribution and size and are therefore generally more applicable than non-ordered mesoporous carbon, which lacks both characteristics [8]. Regardless of the specific type of MCM synthesized, the narrow range of pore sizes allows for a great amount of control of various characteristics during synthesis, as the limited range will only allow very specialized characteristics to emerge. Other unique properties of mesoporous carbon include thermal, mechanical, and electrical stability; chemical inertness; ordered pore structure; and large surface area and pore volume, all of which can be influenced by the specific pore size [5–10].

The unique properties of MCMs allow for a variety of uses for both everyday and scientific purposes. These materials are capable of being used as electrode materials for fuel cells and batteries, absorbents for biomolecules and dyes, framework templates for other nanostructures, and even reaction catalysts [8–11]. Furthermore, factors like cost, complexity of synthesis, and potential wasted materials can be reduced by using MCMs as opposed to traditional catalysts, as MCMs are only made of ordered carbon atoms that are synthesized via well-established procedures [8].

One such method of synthesizing MCMs involves filling mesoporous silica with a carbon precursor, commonly sucrose, which then undergoes several high-temperature processes. The silica backbone is then removed with hydrofluoric acid, with the resulting carbon being highly ordered with specific pore volumes and sizes [12]. Unfortunately, this process involves highly aggressive chemicals that, along with intermediary products, end up becoming potentially dangerous waste. However, one novel method of forming MCM's has recently been developed that significantly decreases the environmental impact of production. This method involves using starches, corn starches in this case, and expanding the present pores to increase the catalytic potential [13]. Starches are typically rather high-density substances, which makes them ideal for chromatography, but catalytically, they are rather inert. By expanding the pores, not only was the catalytic activity of the starch significantly increased, but the properties of the starch were also maintained [13]. Furthermore, the pore sizes and properties can be manipulated simply by altering the temperature used for pore expansion, allowing in precise pore volume control [14]. A similar process has also been conducted on other plant fibers, with similar results [12]. The

benefits of this new method include the starting material being renewable, the lack of toxic materials needed for the reaction, and the ease of synthesis [12,13,15].

In terms of the properties of MCMs, which allow them to excel as catalysts, all the properties previously stated help to give mesoporous carbon the benefit over traditional catalysts. Despite the unsuccessful attempts to finely control the porosity of mesoporous carbon, which has either resulted in larger-than-desired pores or a lack of diameters, it is known that the pores are a major factor in dictating what reactions the MCMs can catalyze [5,16]. It is also known that volume and surface area are directly related to pore size, as mathematically, larger pores give less volume and, depending on other factors, more surface area. The general morphology of the catalyst mainly dictates the orientation necessary for the most efficient catalytic route. The selection of the catalyst shape, with a common shape being a "sieve", allows the catalyst to align itself to fit more possible catalytic sites than a traditional catalyst; this could be due to the flexibility of the material [6]. Finally, the stability of the catalyst dictates how reusable a catalyst is, how reproducible the results of the catalysis are, and how well it can handle certain substances like oxygen or methanol [17,18]. However, despite these benefits of MCMs, there are still means to improve them, with one such way being the implementation of metal nanoparticles.

Nanomaterials are materials with at least one dimension measuring between 1 nm and 100 nm. Nanoparticles and nanofilms are examples of 1D and 2D nanomaterials, respectively, and have been the focus of scientific study due to their unique properties [19,20]. However, it is difficult to control the performance of nanoparticles in reactions, as the performance depends greatly on their characteristics, such as shape, size, crystal structure, and texture [21–24]. Even nanoparticles of noble metals, which are metals that resist chemical reactions and are relatively inert at the bulk level, still possess these inherent downsides to some degree. Nanoparticles have much potential as inorganic catalysts, but due to these difficulties in controlling their performance, their stability is debatable. Specifically, in regard to catalysis, metal nanoparticles show great promise due to their large surface area and overall catalytic capabilities, but they easily agglomerate when catalyzing a reaction. When nanoparticles agglomerate, they stick together to form significantly larger metal chunks. During this process, these larger pieces of metal lose their increased surface area and thus their catalytic capabilities [25]. In order to remedy this issue, the nanoparticles will be imbedded within mesoporous carbon to both prevent the agglomeration of the nanoparticles, but also to take advantage of the catalytic activity of both materials.

By implementing nanoparticles into mesoporous carbon (NP-MCM), forming a nanocomposite, the mesoporous carbon can act as a framework for the nanoparticles to settle in, allowing for the nanoparticles to take the shape of the pores and thus gain control of the properties that alter their performance [21,26]. Other attempts have been made to finely control the size and shape of nanoparticles, such as hydrogen reduction, self-assembly, and a porous support matrix, but none have shown consistent results [21]. By taking control of the exact size, shape, structure, and texture of the nanoparticles, and preventing them from changing by forming a nanocomposite, the issue of the stability of the nanoparticles could be mitigated. Another potential strategy for implementing nanoparticles into mesoporous carbon involves making a mesoporous carbon capsule, in which the nanoparticles are free to move within, coined "Nanorattle", but this is a somewhat outdated strategy that does not allow for as much fine control [27].

Precious metal nanoparticles such as gold and silver (AuNP and AgNP, respectively) are known for their catalytic capabilities and their selective nature [7,21–23,26]. These two metals are part of a larger group of metals known as "Noble Metals", which, on the bulk scale, are generally unreactive. However, when made into nanoparticles, these metals become highly catalytically active and require a low energy cost, with the unreactive nature translating into a form of selectivity that allows for the catalysis of specific reactions [21–23,26–30]. Silver in particular is size- and shape-dependent, capable of forming smaller particles with a large surface area that allows for a facilitated electron flow [21,28]. Furthermore, silver is known for having antibacterial effects and insignificant cytotoxic-

ity, so the silver nanoparticles would be capable of preventing contamination during the catalysis [22,31]. Silver nanoparticles have also been utilized in a number of reactions as catalysts [32–35]

This study was designed to synthesize a nanocomposite catalyst that is highly active, stable, and easily recyclable by embedding silver nanoparticles in mesoporous carbon. Since both mesoporous carbon and metal nanoparticles possess catalytic properties, synthesizing a nanocomposite of the two could result in a stable catalyst that has far greater catalytic abilities than either one alone. This Ag-MCM nanocomposite was tested for catalytic activity in hydrogen evolution reduction reactions from $NaBH_4$, where the concentration of $NaBH_4$, pH, and temperature were varied in order to determine the optimum parameters. The Ag-MCM nanocomposite was also characterized via TEM, XRD, and SEM-EDS.

2. Experimental

2.1. Synthesis

The mesoporous carbon was synthesized from corn starch. In summary, cornstarch is heated in water until gelatinized, which occurs in the temperature range of 350–600 °C, and is then cooled, forming a porous gel. This gel is then treated with ethanol and acetone, and is then dried for up to 2 days, yielding a mesoporous starch. The starch is then treated with 1 mmol of organic acid per gram of starch and is heated, resulting in the final MCM product [12–14]. Silver nanoparticles were synthesized by preparing 100 mL of a 1 mM precursor solution of silver nitrate and heating it to a boil. A 1% *w/w* sodium citrate solution was made, with 5 mL being added to the silver nitrate solution. The solution continued to boil until a color change was observed, and it was cooled [36]. The Ag-MCM nanocomposite was synthesized by adding 40 mL of the precursor solution to one gram of mesoporous carbon in order to functionalize the mesoporous carbon via the incipient wetness impregnation method [26]. The resulting mixture was then dried in an oven at 50 °C until no liquid remained.

2.2. Characterization

Transmission Electron Microscopy (TEM, JEM-2100F, JEOL, Akishima, Tokyo, Japan) was used to visualize the size of the nanoparticles in the composite and to characterize the binding between the nanoparticles and the mesoporous carbon. X-ray Diffraction (XRD, Rigaku Miniflex II, Cu Kα X-ray, nickel filters, Rigaku, Tokyo, Japan) was used to determine the crystallinity structure of mesoporous carbon and its composite. An acquisition rate of 5° min^{-1} with a step size of 0.02° was chosen.

Scanning Electron Microscopy/Energy-Dispersive Spectroscopy (SEM, JEOL JSM-6060LV/EDS, JEOL, Akishima, Tokyo, Japan; ThermoScientific UltraDry , Thermo Fischer Scientific, Waltham, Massachusetts, USA) was used to determine the elemental composition of the nanocomposite and to further confirm the presence of nanoparticles on the mesoporous carbon. The sample, in a powder form, was mounted on a sample holder with carbon tape and analyzed under FE-SEM with an EDAX attachment. Images were taken at different magnifications and at an accelerating voltage of 15 kV.

2.3. Catalytic Tests

The catalytic properties of the nanocomposite were tested using a hydrogen evolution reduction reaction, with sodium borohydride ($NaBH_4$) as the reducing agent, and determining the peak hydrogen generated using a gravimetric water displacement system [37]. This displacement system involves a series of Buchner flasks connected via plastic tubing. Both flasks were filled with 100 mL of deionized water, with one flask being designated as the reaction vessel. The second flask was sealed with a rubber stopper, through which more tubing led to a plastic cup resting on an electronic balance (Ohaus Pioneer Balance (Pa124, OHAUS, Parsippany, NJ, USA) with proprietary mass logging software, OHAUS, Parsippany, NJ, USA, V2.04). A catalytic trial began by adding both $NaBH_4$ and the catalyst to the reaction vessel, which was then sealed with a rubber stopper. As the reaction

produced hydrogen gas, the reaction vessel would fill with hydrogen gas. The gas then flowed through the tubing connecting the two flasks and filled the second flask, at which point it would pour water out of the flask and into the cup on the balance. The volume of hydrogen generated from the reaction could be determined according to the volume of water displaced into the cup. To determine the optimal condition for the reaction to occur, the concentration of $NaBH_4$ (0.00079 mol, 0.00095 mol, and 0.00106 mol) was varied, the pH (6, 7, and 8) was varied, and the temperature (273 K, 288 K, 295 K, and 303 K) was varied [37]. In all trials, 0.01 g of the Ag-MCM nanocomposite catalyst was used and 100 mL of deionized water was used in all $NaBH_4$ solutions. During the reaction, the solution was stirred with a magnetic stir bar to maintain the suspension of the Ag-MCM [37]. Each variation was repeated twice, with third trials performed as necessary.

2.4. Catalyst Reusability

In order to test the reusability of the Ag-MCM nanocomposites, a 0.00095 mol solution of $NaBH_4$ and 100 mL of deionized water at pH 7 and 295 K was made, and 0.01 g of the nanocomposite was added [37]. The same solution containing the deionized water and the catalyst was used in four additional reactions, adding 0.01 g more of $NaBH_4$ for each trial, for a total of 5 trials.

3. Results/Discussions

3.1. Catalyst Characterization

The TEM micrographs seen in Figure 1 shows silver nanoparticles embedded within the mesoporous carbon material. The silver nanoparticles vary in diameter, possessing diameters of 50 nm and larger. The SEM/EDS analysis in Figure 2 helped to confirm that the nanoparticles seen were in fact made of silver.

The presence of silver within our composite was further confirmed using the XRD spectra (Figure 3). The presence of sharp peaks in the 24° and 40° range seen in the MCM material are correlating to the carbon. These peaks are shifted up in the Ag-MCM composite, indicating a change in the lattice structure [38]; this is likely due to the addition of AgNPs. Peaks were observed at 40, 44.7, and 66.6 degrees representing the (111), (200), and (220) faces of the face centered cubic (FCC) silver nanoparticles (JCPDS 65-2871). The inset figure in Figure three highlights the (220) peak at 66.6 degrees, which exhibits a lower intensity compared to the highly intense carbon peak.

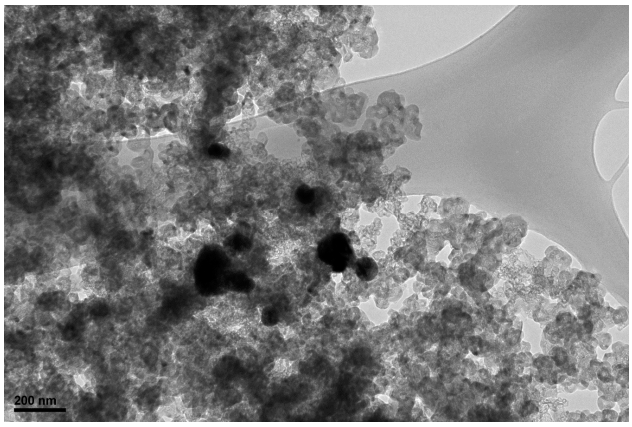

(**A**)

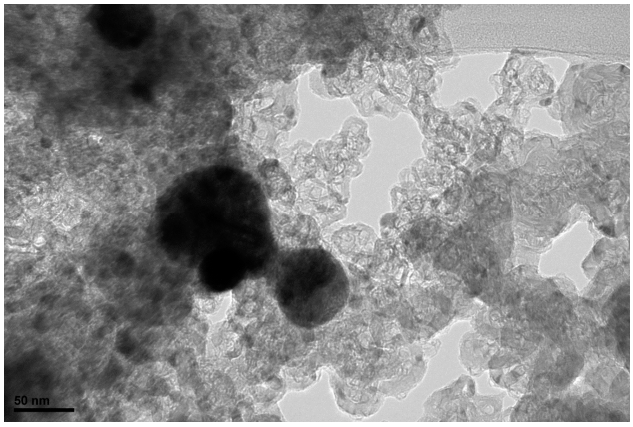

(**B**)

Figure 1. TEM images of the Ag-MCM catalyst at magnifications of (**A**) 200 nm and (**B**) 50 nm.

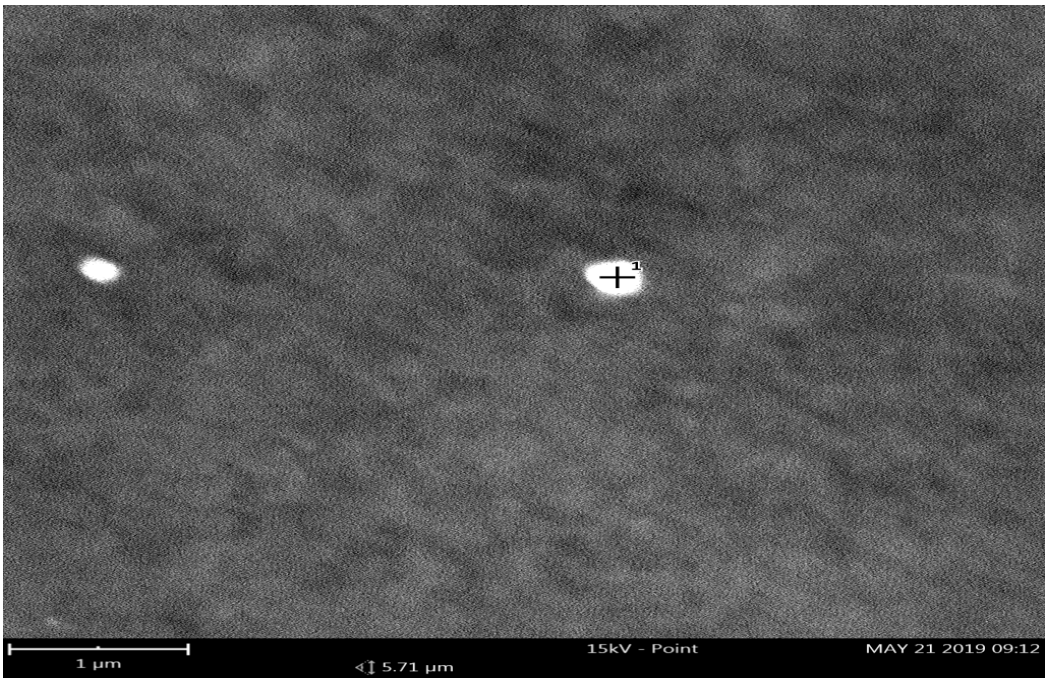

(**a**)

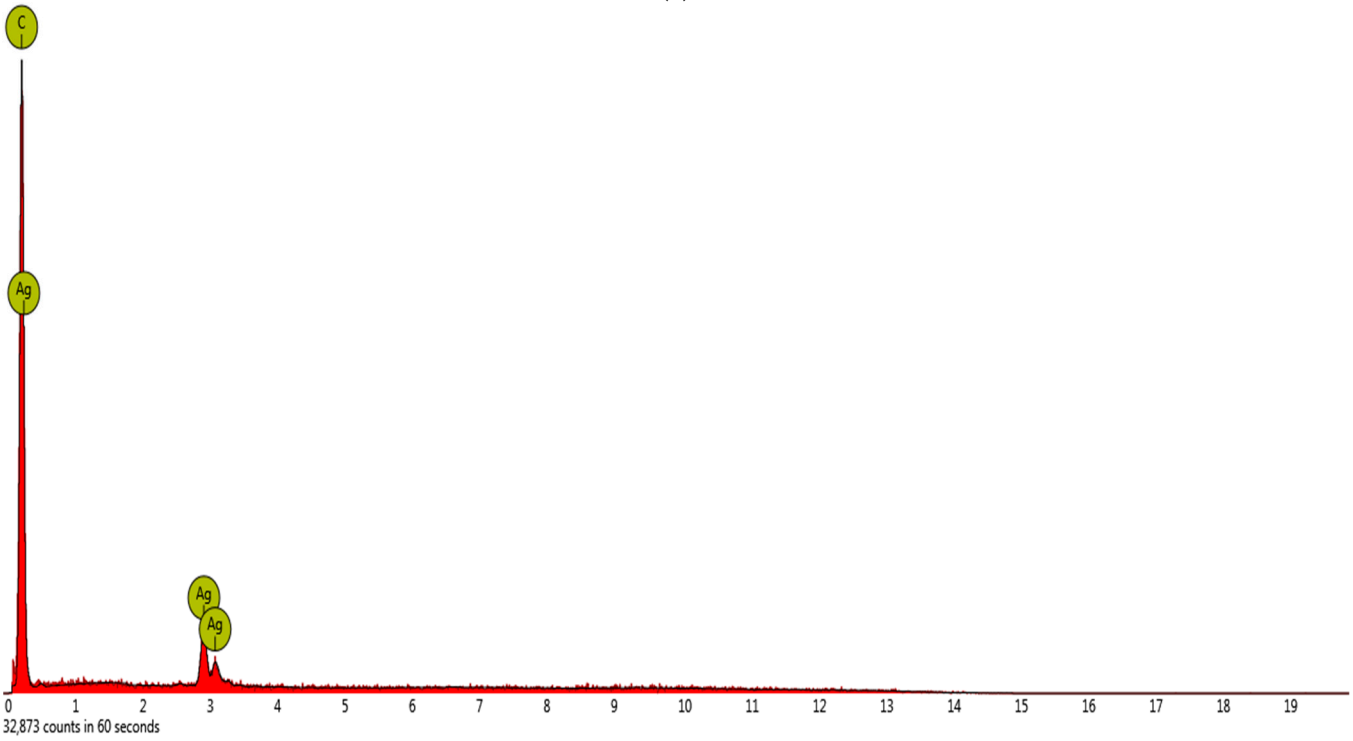

(**b**)

Figure 2. SEM/EDX analysis with (**a**) the SEM micrograph of the Ag-MCM catalyst and (**b**) the EDS spectrum correlating to the indicated silver nanoparticle.

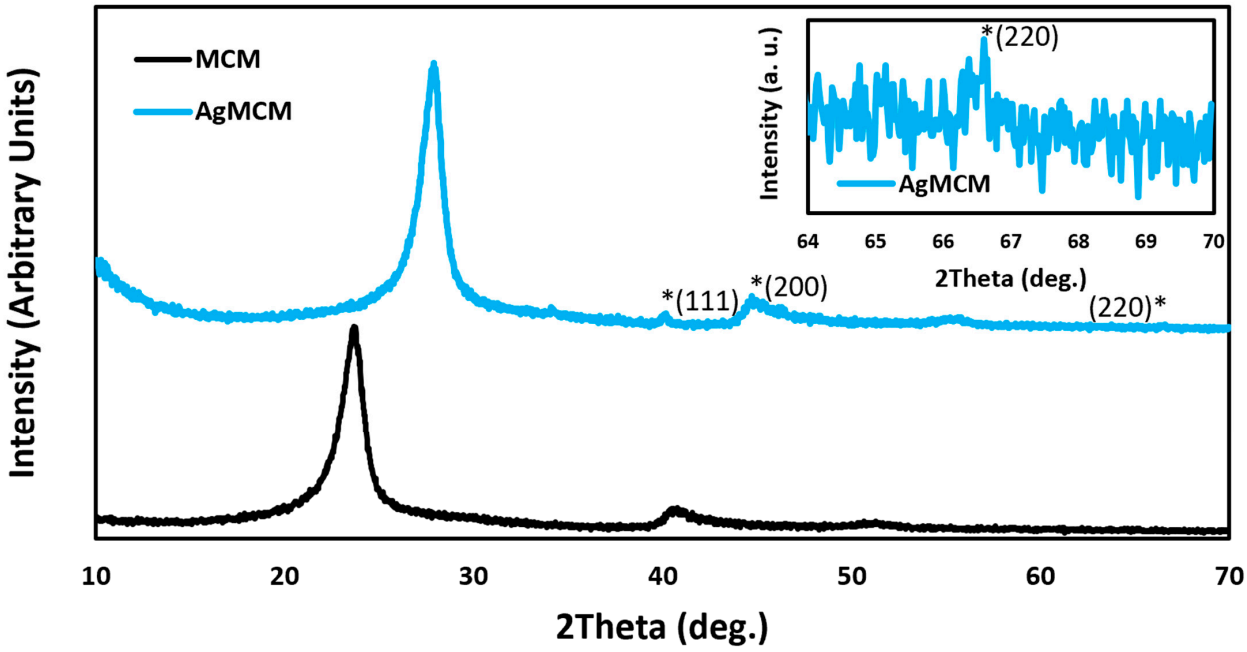

Figure 3. XRD spectra for the Ag-MCM catalyst and MCM without AgNPs scanned at 0.5 degrees per minute for 90 degrees. The inset graph highlights the (220) lattice face of the silver nanoparticles.

3.2. Catalytic Tests

Our Ag-MCM catalyst was tested for its catalytic ability under various conditions. The first condition tested was the concentration of $NaBH_4$ used during the reaction (Figure 4). For reactions tested at 0.00079 mol, an average hydrogen production rate of 0.011 mL min^{-1} mg^{-1} was observed, producing an average volume of 12.9 mL after 120 min. For 0.00095 mol, the production rate was determined to be 0.015 mL min^{-1} mg^{-1}, with an average volume of 17.9 mL. Lastly, when 0.00106 mol was tested, the amount of hydrogen generated was found to be 42.1 mL and the production rate was found to be 0.035 mL min^{-1} mg^{-1}. Based on these results, it is clear that an increase in the concentration of $NaBH_4$ used during this reaction results in an increase in the amount of hydrogen produced. This is in agreement with Equation (2) and Le Chatlier's principle.

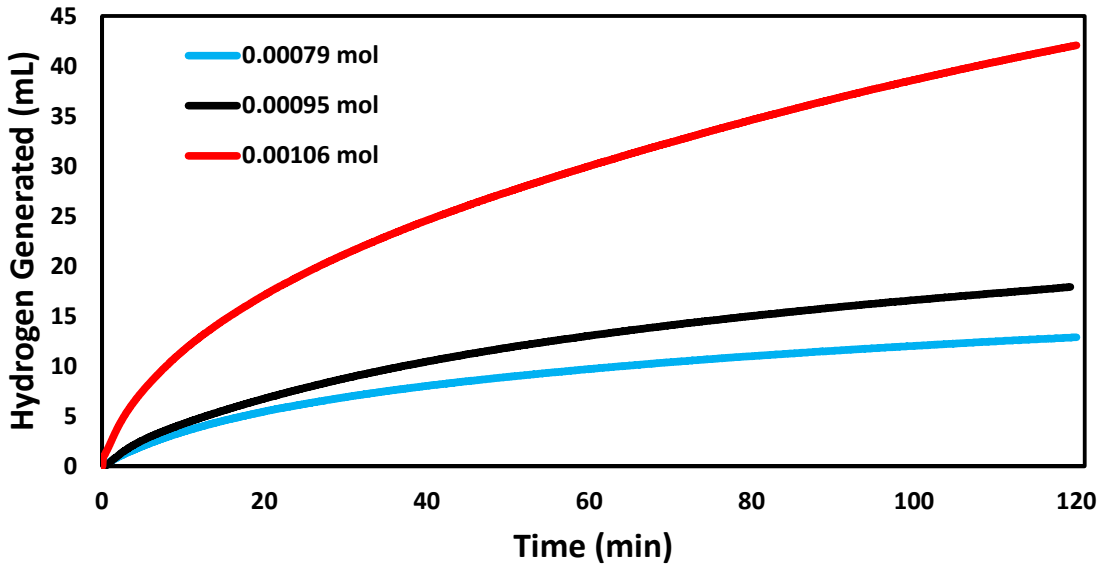

Figure 4. Hydrogen generated (mL) vs. time (min) under varying concentrations of $NaBH_4$.

Next, the reaction was tested under acidic conditions (pH 6), basic conditions (pH 8), and compared to ambient conditions (pH 7) (Figure 5). It was found that the reaction produces the most hydrogen when the pH is 6, with a production rate of 0.035 mL min^{-1} mg^{-1} and an average volume of hydrogen produced of 42.1 mL. This is in accordance with the previous literature that states that acidic conditions increase the amount of hydrogen ions that can react to product diatomic hydrogen [39]. It was observed that increasing the pH of the reaction to 8 resulted in less hydrogen being produced with an average rate of 0.010 mL min^{-1} mg^{-1} and a volume of 12.6 mL. This is in agreement with previous work within this team and also with the work of Kaufman et al. [25,36,40–44].

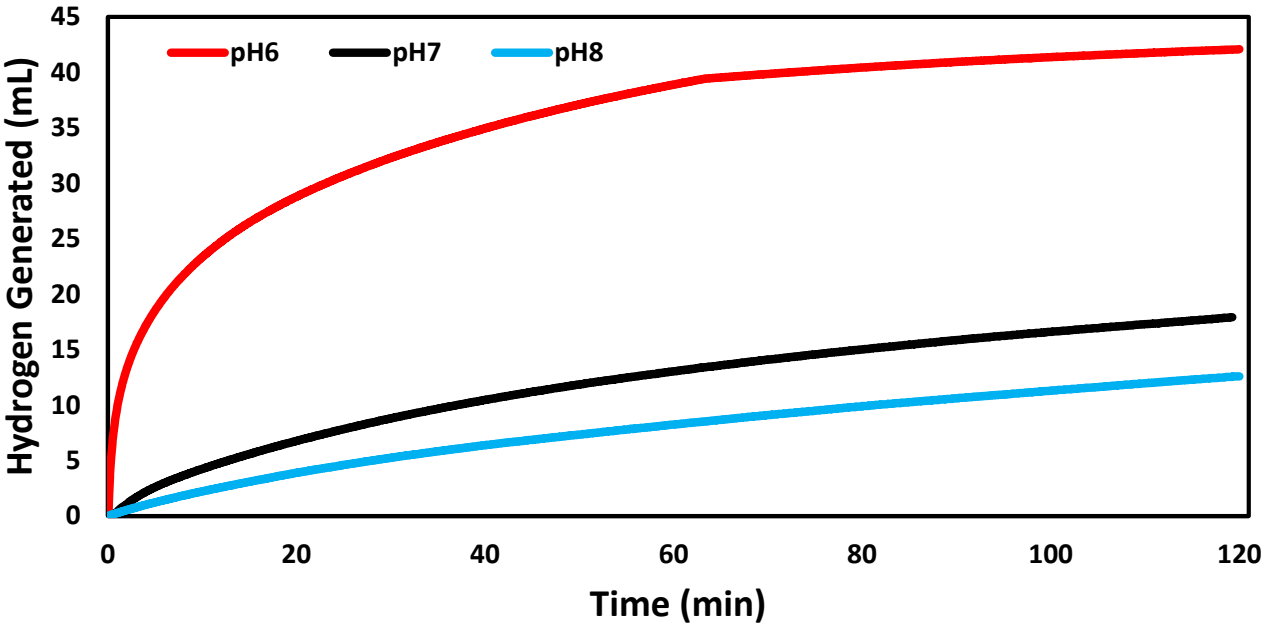

Figure 5. Hydrogen generated (mL) vs. time (min) under varying pH conditions.

The catalytic ability of our Ag-MCM was then tested at multiple different temperatures, as seen in Figure 6. First, the reaction was tested at 0 °C or 273 K, which produced an average volume of 11.8 mL at a rate of 0.010 mL min^{-1} mg^{-1}. Next, a hydrogen production rate of 0.012 mL min^{-1} mg^{-1} and an average volume of 14.2 mL was seen at the temperature of 15 °C (288 K). Room temperature trials (295 K) resulted in an average volume of 18.1 mL and a rate of 0.014 mL min^{-1} mg^{-1}. Lastly, when tested at 30 °C (or 303 K), the rate of production was observed to be 0.020 mL min^{-1} mg^{-1}, producing an average volume of 23.8 mL after 2 h. A direct correlation between temperature and the amount of hydrogen produced was seen, with hotter temperatures producing more hydrogen. Based on Le Chatelier's principle and Equation (2), this tells us that the reaction is an endothermic reaction.

After the temperature trials, the calculated rate constants were used with Equation (3) to create an Arrhenius plot (Figure 7).

$$k = Ae^{-\frac{Ea}{RT}} \quad (3)$$

In Equation (3), k is the rate constant at a tested temperature, A is the pre-exponential factor, Ea is the activation energy of the reaction, R is the universal gas constant, and T is the absolute temperature.

Figure 7 was used in order to determine that the activation energy of our catalyst was 15.6 kJ mol^{-1}. When compared to other catalysts for this reaction (Table 1), Ag-MCM is incredibly low. When compared to other precious metal composites, Ag-MCM greatly outperforms Ru/Graphite, Pd/C, and Ru/C. The Ea of Ag-MCM is also much lower than the other composites explored within this team, such as Au/MWCNTs, Pd/MWCNTs,

BCD-AuNP, and PtNPs. Other catalysts that came close to ours include $CoCl_2$, Silica sulfuric acid, and Pt–Pd/CNTs. Even when compared to another composite that used silver (Ag/MWCNTs), this Ag-MCM composite shows an improved catalytic ability.

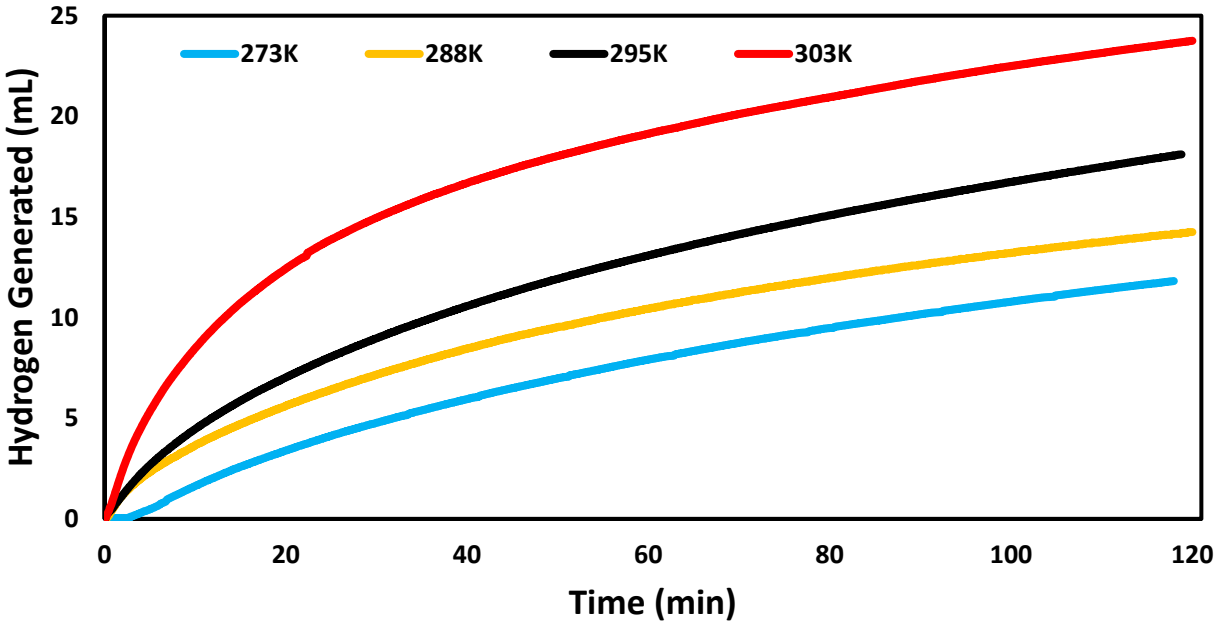

Figure 6. Hydrogen generated (mL) vs. time (min) under varying temperatures.

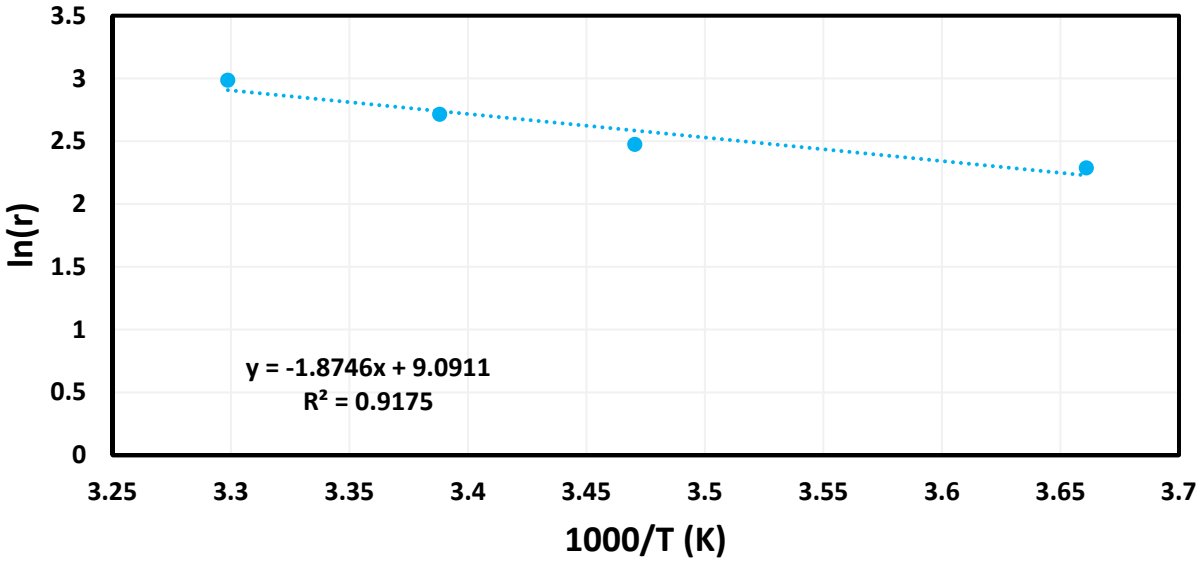

Figure 7. Arrhenius plot made from the natural log of the reaction rate vs. 1000 over the temperature in Kelvin.

Table 1. Comparison of reported activation energies for catalyzed $NaBH_4$ hydrolysis.

Catalyst	E_a (kJ mol^{-1})	Temperature (K)	Reference
MWCNT supported Co	40.4	298–333	[45]
Co-B	64.9	283–303	[46]
$CoCl_2$	17.5	293–308	[47]
Silica sulfuric acid	17	298–343	[48]
Ru/Graphite	61.1	398–318	[49]
Ru/C	67	298–358	[50]

Table 1. *Cont.*

Catalyst	E_a (kJ mol^{-1})	Temperature (K)	Reference
Pd/C	28	298–328	[51]
Pt–Pd/CNTs	19	302–332	[52]
Au/MWCNTs	21.1	273–303	[26]
Ag/MWCNTs	44.5	273–303	[41]
Pd/MWCNTs	62.7	273–303	[42]
BCD-AuNP	54.7	283–303	[43]
PtNPs	39.2	283–303	[44]
PtFCS	53.0	283–303	[53]
AgNP-FCS	37.0	273–303	[54]
PdFGLM	45.1	283–303	[55]
AuFGLM	45.5	283–303	[56]
CuGLM	46.8	283–303	[57]
Ag-MCM	15.6	273–303	This Work

3.3. Catalytic Reusability Tests

The Ag-MCM catalyst underwent reusability trials to determine how reusable it was after five consecutive trials, with conditions involving 952 µmol of $NaBH_4$, a pH of 7, and a temperature of 295 K (Figure 8). Hydrogen generation remained relatively consistent, with the average hydrogen generated after two hours for the five trials being determined to be 20.0 mL. Despite the consistency, there was a slight increase observed towards the later trials, possibly indicating that the catalyst becomes more activated after several trials. It has been previously reported that as the concentration of BH_4^- ions increases in the solution, bonds form between the ions and the surface of the nanoparticles. This increases the electrostatic stability of the nanoparticles surface, increasing their catalytic ability [58].

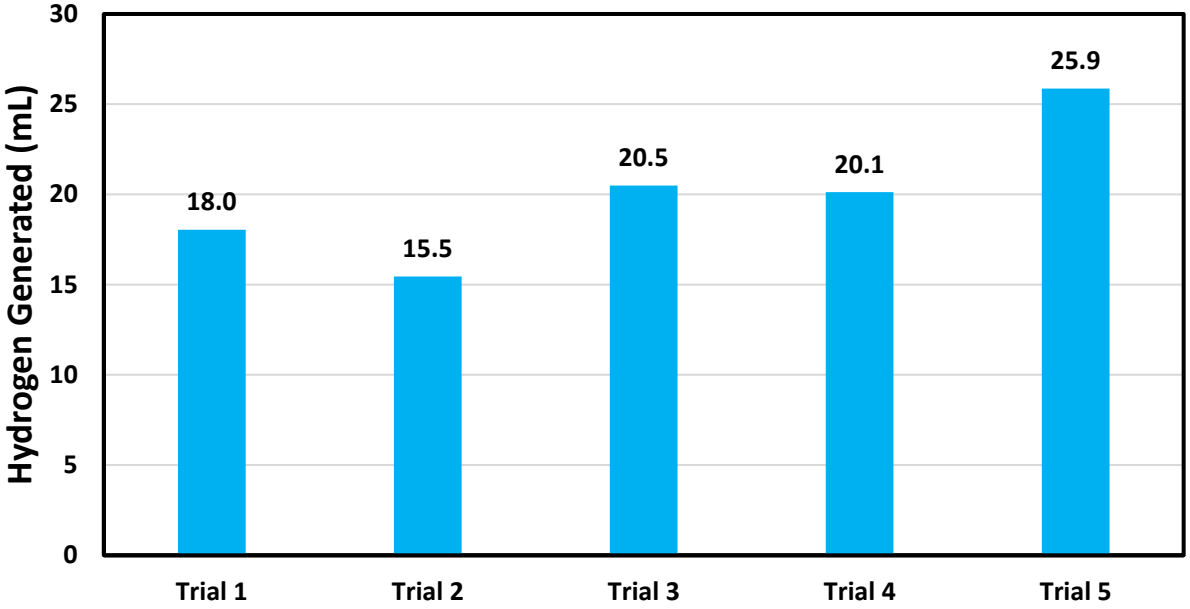

Figure 8. Testing reusability of the Ag-MCM catalyst after five consecutive hydrogen generation reactions.

Scheme 1 depicts a possible route of hydrogen generation via the water splitting reaction of $NaBH_4$ with the Ag-MCM catalyst. After $NaBH_4$ dissociates in water, a free borohydride ion [BH_4^-] adheres itself to a AgNP on the MCM backbone. A water molecule will then attack the borohydride, stripping a hydrogen and leaving a hydroxyl group in its place. This can happen three additional times, resulting in a total of four diatomic hydrogen molecules released [$4H_2$]. After the fourth attack, the remaining tetrahydroxyborate ion

$[B(OH)_4^-]$ detaches from the AgNP, allowing a new BH_4^- to take its place and repeat the cycle [59].

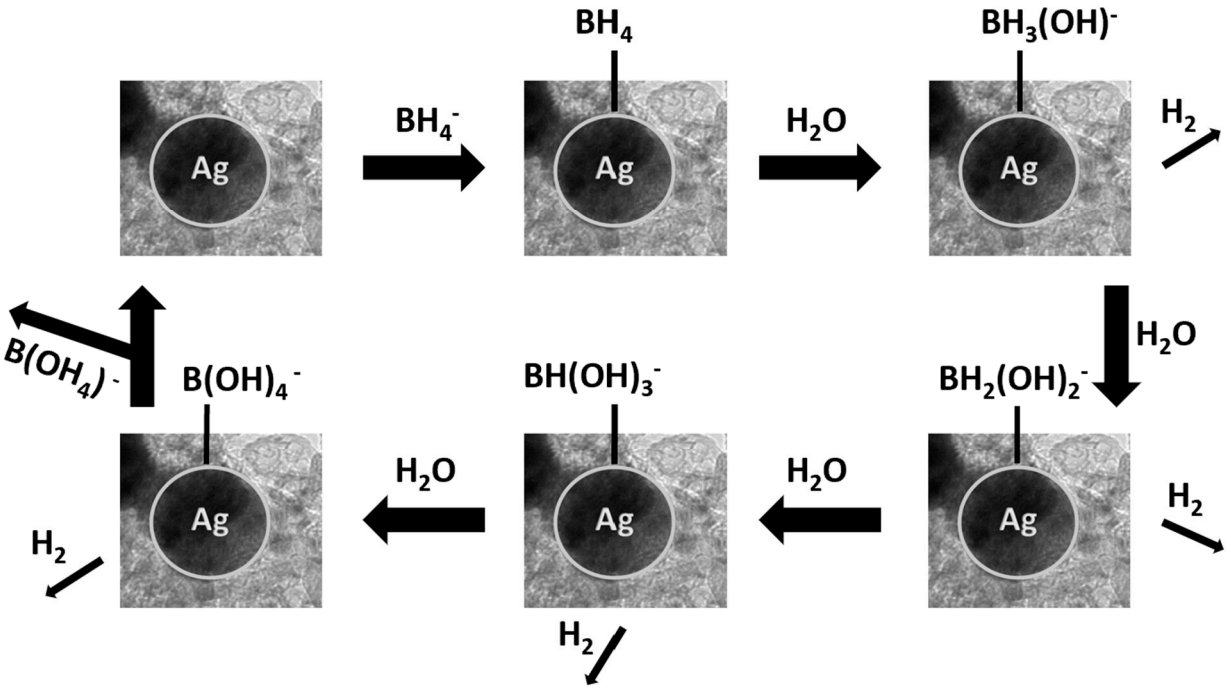

Scheme 1. Mechanism for the Ag-MCM-catalyzed hydrolysis of $NaBH_4$.

4. Conclusions

The synthesized mesoporous carbon catalyst was characterized via Transmission Electron Microscopy (TEM), Scanning Electron Microscopy/Energy-Dispersive Spectroscopy (SEM/EDS), and X-ray Diffraction (XRD). The catalytic activity of Ag-MCM was found to be enhanced by increased temperatures, concentrations of $NaBH_4$, and lower pHs, while the opposites of those conditions impeded the catalytic ability. The activation energy of this catalyst was found to be impressively low at 15.6 kJ mol^{-1}, which, when compared to activation energies of other similar catalysts, is one of the lowest reported for this reaction. Catalytic reusability tests of these catalysts indicated that the Ag-MCM catalyst was generally stable, as it was capable of producing consistent amounts of hydrogen gas even after five consecutive trials, with even a possible increase in H_2 with later uses. Not only does this material prove to be an excellent catalyst, but it also utilizes a cheap and readily available MCM support that is derived from sustainable cornstarch, relatively mild synthesis conditions, and mild reaction conditions.

Author Contributions: Conceptualization, T.M.A.-F.; Validation, T.M.A.-F.; Investigation, E.B.; Resources, T.M.A.-F.; Data curation, E.B. and Q.Q.; Writing—original draft, E.B.; Writing—review & editing, Q.Q. and T.M.A.-F. All authors have read and agreed to the published version of the manuscript.

Funding: This research received no external funding.

Data Availability Statement: The original contributions presented in the study are included in the article, further inquiries can be directed to the corresponding author.

Acknowledgments: The corresponding author acknowledges Lawrence J. Sacks' professorship in chemistry.

Conflicts of Interest: The authors declare no conflict of interest.

References

1. World Energy Council. *World Energy Resources 2016 Report*; Report No. 24; World Energy Council: London, UK, 2016.
2. Shafiee, S.; Topal, E. When will fossil fuel reserves be diminished? *Energy Policy* **2008**, *37*, 181–189. [CrossRef]
3. Raupach, M.R.; Marland, G.; Ciais, P.; Le Quéré, C.; Canadell, J.G.; Klepper, G.; Field, C.B. Global and regional drivers of accelerating CO_2 emissions. *Proc. Natl. Acad. Sci. USA* **2007**, *104*, 10288–10293. [CrossRef] [PubMed]
4. Veziroglu, T.N. 21st Century's Energy: Hydrogen Energy System. *Assess. Hydrog. Energy Sustain. Dev. NAPSC* **2007**, *4*, 9–31. [CrossRef]
5. Xia, Y.; Yang, Z.; Mokaya, R. Simultaneous Control of Morphology and Porosity in Nanoporous Carbon: Graphitic Mesoporous Carbon Nanorods and Nanotubules with Tunable Pore size. *Chem. Mater.* **2005**, *18*, 140–148. [CrossRef]
6. Liang, C.; Li, Z.; Dai, S. Mesoporous Carbon Materials: Synthesis and Modification. *Angew. Chem. Int.* **2008**, *47*, 3696–3717. [CrossRef] [PubMed]
7. Horváth, E.; Puskás, R.; Rémiás, R.; Mohl, M.; Kukovecz, Á.; Kónya, Z.; Kiriesi, I. A Novel Catalyst Type Containing Noble Metal Nanoparticles Supported on Mesoporous Carbon: Synthesis, Characterization and Catalytic properties. *Top Catal.* **2009**, *52*, 1242–1250. [CrossRef]
8. Chang, H.; Joo, S.H.; Pak, C. Synthesis and characterization of mesoporous carbon for fuel cell applications. *J. Mater. Chem.* **2007**, *17*, 3078–3088. [CrossRef]
9. Xia, Y.; Mokaya, R. Generalized and Facile Synthesis Approach to N-Doped Highly Graphitic Mesoporous Carbon Materials. *Chem Mater.* **2005**, *17*, 1553–1560. [CrossRef]
10. Su, F.; Zeng, J.; Bao, X.; Yu, Y.; Lee, J.Y.; Zhao, X.S. Preparation and Characterization of Highly Ordered Graphitic Mesoporous Carbon as a Pt Catalyst Support for Direct Methanol Fuel Cells. *Chem. Mater.* **2005**, *17*, 3960–3967. [CrossRef]
11. Matos, I.; Bernardo, M.; Neves, P.D.; Castanheiro, J.E.; Vital, J.; Fonseca, I.M. Mesoporous Carbon as effective and sustainable catalyst for fine chemistry. *Bol. Grupo Español Carbón* **2016**, *39*, 19–22.
12. Budarin, V.; Clark, J.H.; Hardy, J.J.E.; Luque, R.; Milkowski, K.; Tavener, S.J.; Wilson, A.J. Starbons: New Starch-Derived Mesoporous Carbonaceous Materials with Tunable Properties. *Angew. Int. Ed.* **2007**, *45*, 3782–3786. [CrossRef] [PubMed]
13. Biehler, E.; Quach, Q.; Abdel-Fattah, T. Screening study of Different Carbon Based Materials for Hydrogen. *ECS J. Solid State Sci. Technol.* **2023**, *12*, 081002. [CrossRef]
14. Shuttleworth, P.S.; Budarin, V.; White, R.J.; Gun'ko, V.M.; Luque, R.; Clark, J.H. Molecular-Level Understanding of the Carbonisation of Polysaccharides. *Chem. Eur. J.* **2013**, *19*, 9351–9357. [CrossRef] [PubMed]
15. Milkowski, K.; Clark, J.H.; Doi, S. New materials based on renewable resources: Chemically modified highly porous starches and their composites with synthetic monomers. *Green Chem.* **2004**, *6*, 189–190. [CrossRef]
16. Hussain, M.; Ihm, S. Synthesis, Characterization, and Hydrodesulfurization Activity of New Mesoporous Carbon Support Transition Metal Sulfide Catalysts. *Ind. Eng. Chem. Res.* **2009**, *48*, 698–707. [CrossRef]
17. Gupta, G.; Slanac, D.A.; Kumar, P.; Wiggins-Camacho, J.D.; Kim, J.; Ryoo, R.; Stevenson, K.J.; Johnston, K.P. Highly Stable Pt/Ordered Graphitic Mesoporous Carbon Electrocatalysts for Oxidation Reduction. *J. Phys. Chem. C* **2010**, *114*, 10796–10805. [CrossRef]
18. Wen, Z.; Liu, J.; Li, J. Core/Shell Pt/C Nanoparticle Embedded in Mesoporous Carbon as a Methanol-Tolerant Cathode Catalyst in Direct Methanol fuel Cells. *J. Adv. Mater.* **2008**, *20*, 743–747. [CrossRef]
19. Kholoud, M.M.; El-Nour, A.; Eftaiha, A.; Al-Warthan, A.; Ammar, R.A.A. Synthesis and applications of silver nanoparticles. *Arabian J. Chem.* **2010**, *3*, 135–140.
20. Dushatinski, T.; Huff, C.; Abdel-Fattah, T.M. Characterization of electrochemically deposited films from aqueous and ionic liquid cobalt precursors toward hydrogen evolution reactions. *Appl. Surf. Sci.* **2016**, *385*, 282–288. [CrossRef]
21. Datta, K.K.R.; Reddy, B.V.S.; Ariga, K.; Vinu, A. Gold Nanoparticles Embedded in a Mesoporous Carbon Nitride Stabilizer for Highly Efficent Three-Component Coupling Reaction. *Angew. Chem.* **2010**, *122*, 6097–6101. [CrossRef]
22. Gan, X.; Liu, T.; Zhong, J.; Li, G. Effect of Silver Nanoparticles on Electron Transfer Reactivity and the Catalytic Activity of Myoglobin. *ChemBioChem* **2004**, *5*, 1686–1691. [CrossRef] [PubMed]
23. Xu, R.; Wang, D.; Zhang, J.; Li, Y. Shape-Dependent Catalytic Activity of Silver Nanoparticles for the Oxidation of Styrene. *Chem. Asian J.* **2006**, *1*, 888–893. [CrossRef] [PubMed]
24. Beck, J.S.; Vartuli, J.C.; Roth, W.J.; Leonowicz, M.E.; Kresge, C.T.; Schmitt, K.D.; Chu, C.T.W.; Olson, D.H.; Sheppard, E.W.; McCullen, S.B.; et al. A new family of mesoporous molecular sieves prepared with liquid crystal templates. *J. Am. Chem. Soc.* **1992**, *114*, 10834–10843. [CrossRef]
25. Comotti, M.; Pina, C.D.; Matarrese, R.; Rossi, M. The Catalytic Activity of "Naked" Gold Particles. *Angew. Chem. Int. Ed.* **2004**, *43*, 5812–5815. [CrossRef] [PubMed]
26. Huff, C.; Dushatinski, T.; Abdel-Fattah, T.M. Gold nanoparticle/multi-walled carbon nanotube composite as novel catalyst for hydrogen evolution reactions. *Int. J. Hydrogen Energy* **2017**, *42*, 18985–18990. [CrossRef]
27. Kim, M.; Sohn, K.; Bin Na, H.; Hyeon, T. Synthesis of Nanorattles Composed of Gold Nanoparticles Encapsulated in Mesoporous Carbon and Polymer Shells. *Nano Lett.* **2002**, *2*, 1383–1387. [CrossRef]
28. Liang, M.; Su, R.; Qi, W.; Yu, Y.; Wang, L.; He, Z. Synthesis of well-dispersed Ag nanoparticles on eggshell membrane for catalytic reduction of 4-nitrophenol. *J. Mater. Sci.* **2014**, *49*, 1639–1647. [CrossRef]

29. Lopez, N.; Janssens, T.V.W.; Clausen, B.S.; Xu, Y.; Mavrikakis, M.; Bligaard, T.; Nørskov, J.K. On the origin of the catalytic activity of gold nanoparticles for low-temperature CO oxidation. *J. Catal.* **2004**, *223*, 232–235. [CrossRef]
30. Daté, M.; Okumura, M.; Tsubota, S.; Haruta, M. Vital Role of Moisture in the Catalytic Activity of Supported Gold Nanoparticles. *Angew. Chem. Int. Ed.* **2004**, *43*, 2129–2132. [CrossRef]
31. Seo, Y.; Hwang, J.; Kim, J.; Jeong, Y.; Hwang, M.P.; Choi, J. Antibacterial activity and cytotoxicity of multi-walled carbon nanotubes decorated with silver nanoparticles. *Int. J. Nanomed.* **2014**, *9*, 4621–4629.
32. Sudrik, S.G.; Chaki, N.K.; Chavan, V.B.; Chavan, S.P.; Chavan, S.P.; Sonawane, H.R.; Vijayamohanan, K. Silver Nanocluster Redox-Couple-Promoted Nonclassical Electron Transfer: An Efficient Electrochemical Wolff Rearrangement of α-Diazoketones. *Chem.—Eur. J.* **2006**, *12*, 859–864. [CrossRef] [PubMed]
33. Mitsudome, T.; Mikami, Y.; Mori, H.; Arita, S.; Mizugaki, T.; Jitsukawa, K.; Kaneda, K. Supported Silver Nanoparticle Catalyst for Selective Hydration of Nitriles to Amides in Water. *Chem. Commun.* **2009**, *2009*, 3258. [CrossRef] [PubMed]
34. Mitsudome, T.; Mikami, Y.; Funai, H.; Mizugaki, T.; Jitsukawa, K.; Kaneda, K. Oxidant-Free Alcohol Dehydrogenation Using a Reusable Hydrotalcite-Supported Silver Nanoparticle Catalyst. *Angew. Chem. Int. Ed.* **2008**, *47*, 138–141. [CrossRef] [PubMed]
35. Huff, C.; Long, J.M.; Abdel-Fattah, T.M. Beta-cyclodextrin-assisted synthesis of silver nanoparticle network and its application in a hydrogen generation reaction. *Catalysts* **2020**, *10*, 1014. [CrossRef]
36. Pillai, Z.S.; Kamat, P.V. What Factors Control the Size and Shape of Silver Nanoparticles in the Citrate Ion Reduction Method? *J. Phys. Chem. B* **2004**, *108*, 945–951. [CrossRef]
37. Huff, C.; Dushatinski, T.; Barzanji, A.; Abdel-Fattah, N.; Barzanji, K.; Abdel-Fattah, T.M. Pretreatment of Gold Nanoparticle Multi-Walled Carbon Nanotube Composites for Catalytic Activity toward Hydrogen Generation Reaction. *ECS J. Solid State Sci. Technol.* **2017**, *6*, 69–71. [CrossRef]
38. Antolini, E.; Cardellini, F. Formation of carbon supported PtRu alloys: An XRD analysis. *J. Alloys Compd.* **2001**, *315*, 118–122. [CrossRef]
39. Schlesinger, H.I.; Brown, H.C.; Finholt, A.E.; Gilbreath, J.R.; Hoekstra, H.R.; Hyde, E.K. Sodium borohydride, its hydrolysis and its use as a reducing agent and in the generation of hydrogen. *J. Am. Chem. Soc.* **1953**, *75*, 215–219. [CrossRef]
40. Kaufman, C.M.; Sen, B. Hydrogen Generation by Hydrolysis of Sodium Tetrahydroborate: Effects of Acids and Transition Metals and Their Salts. *J. Chem. Soc. Dalton Trans.* **1985**, *1985*, 307–313. [CrossRef]
41. Huff, C.; Long, J.M.; Aboulatta, A.; Heyman, A.; Abdel-Fattah, T.M. Silver Nanoparticle/Multi-Walled Carbon Nanotube Composite as Catalyst for Hydrogen Production. *ECS J. Solid State Sc.* **2017**, *6*, 115–118. [CrossRef]
42. Huff, C.; Long, J.M.; Heyman, A.; Abdel-Fattah, T.M. Palladium Nanoparticle Multiwalled Carbon Nanotube Composite as Catalyst for Hydrogen Production by the Hydrolysis of Sodium Borohydride. *ACS Appl. Energy Mater.* **2018**, *1*, 4635–4640. [CrossRef]
43. Quach, Q.; Biehler, E.; Elzamzami, A.; Huff, C.; Long, J.M.; Abdel-Fattah, T.M. Catalytic Activity of Beta-Cyclodextrin-Gold Nanoparticles Network in Hydrogen Evolution Reaction. *Catalysts* **2021**, *11*, 118. [CrossRef]
44. Huff, C.; Biehler, E.; Quach, Q.; Long, J.M.; Abdel-Fattah, T.M. Synthesis of Highly Dispersive Platinum Nanoparticles and their Application in a Hydrogen Generation Reaction. *Colloids Surf. A Physicochem. Eng. Asp.* **2020**, *610*, 125734. [CrossRef]
45. Huang, Y.; Wang, Y.; Zhao, R.; Shen, P.K.; Wei, Z. Accurately measuring the hydrogen generation rate for hydrolysis of sodium borohydride on multi-walled carbon nanotubes/Co-B catalysts. *Int. J. Hydrogen Energy* **2008**, *33*, 7110–7115. [CrossRef]
46. Jeong, S.U.; Kim, R.K.; Cho, E.A.; Kim, H.-J.; Nam, S.-W.; Oh, I.-H.; Hong, S.-A.; Kim, S.H. A study on hydrogen generation from $NaBH_4$ solution using the high-performance Co-B catalyst. *J. Power Sources* **2005**, *144*, 129–134. [CrossRef]
47. Levy, A.; Brown, J.B.; Lyons, C.J. Catalyzed Hydrolysis of Sodium Borohydride. *Ind. Eng. Chem.* **1960**, *52*, 211–214. [CrossRef]
48. Manna, J.; Roy, B.; Sharma, P. Efficient hydrogen generation from sodium borohydride hydrolysis using silica sulfuric acid catalyst. *J. Power Sources* **2015**, *275*, 727–733. [CrossRef]
49. Liang, Y.; Dai, H.-B.; Ma, L.-P.; Wang, P.; Cheng, H.-M. Hydrogen generation from sodium borohydride solution using a ruthenium supported graphite catalyst. *Int. J. Hydrogen Energy* **2010**, *35*, 3023–3028. [CrossRef]
50. Zhang, J.S.; Delgass, W.N.; Fisher, T.S.; Gore, J.P. Kinetics of Ru-catalyzed sodium borohydride hydrolysis. *J. Power Sources* **2007**, *164*, 772–781. [CrossRef]
51. Patel, N.; Patton, B.; Zanchetta, C.; Fernandes, R.; Guella, G.; Kale, A.; Miotello, A. Pd-C power and thin film catalysts for hydrogen production by hydrolysis of sodium borohydride. *Int. J. Hydrogen Energy* **2008**, *33*, 287–292. [CrossRef]
52. Peña-Alonso, R.; Sicurelli, A.; Callone, E.; Carturan, G.; Raj, R. A picoscale catalyst for hydrogen generation from $NaBH_4$ for fuel cells. *J. Power Sources* **2007**, *165*, 315–323. [CrossRef]
53. Biehler, E.; Quach, Q.; Abdel-Fattah, T.M. Synthesis of Platinum Nanoparticles Supported on Fused Nanosized Carbon Spheres Derived from Sustainable Source for Application in a Hydrogen Generation Reaction. *Nanomaterials* **2023**, *13*, 1994. [CrossRef]
54. Biehler, E.; Quach, Q.; Abdel-Fattah, T.M. Silver-Nanoparticle-Decorated Fused Carbon Sphere Composite as a Catalyst for Hydrogen Generation. *Energies* **2023**, *16*, 5053. [CrossRef]
55. Quach, Q.; Biehler, E.; Abdel-Fattah, T.M. Synthesis of Palladium Nanoparticles Supported over Fused Graphene-like Material for Hydrogen Evolution Reaction. *Catalysts* **2023**, *13*, 1117. [CrossRef]
56. Biehler, E.; Quach, Q.; Abdel-Fattah, T.M. Gold Nanoparticles AuNP Decorated on Fused Graphene-like Materials for Application in a Hydrogen Generation. *Materials* **2023**, *16*, 4779. [CrossRef] [PubMed]

57. Quach, Q.; Biehler, E.; Abdel-Fattah, T.M. Synthesis of Copper Nanoparticles Supported over Graphene-like Material Composite as a Catalyst for Hydrogen Evolution. *J. Compos. Sci.* **2023**, *7*, 279. [CrossRef]
58. Deraedt, C.; Salmon, L.; Gatard, S.; Ciganda, R.; Hernandez, E.; Ruiz, J.; Astruc, D. Sodium borohydride stabilizes very active gold nanoparticle catalysts. *Chem. Commun.* **2014**, *50*, 14194–14196. [CrossRef] [PubMed]
59. Abdel-Fattah, T.M.; Biehler, E. Carbon Based Supports for Metal Nanoparticles for Hydrogen Generation Reactions Review. *Adv. Carbon J.* **2024**, *1*, 1–19. [CrossRef]